

LEAD-FREE FERROELECTRIC MATERIALS



Lead-free ferroelectric materials: Prospective applications

Shujun Zhang^{1,a)}, Barbara Malič², Jing-Feng Li³, Jürgen Rödel⁴
¹Institute for Superconducting and Electronic Materials, AIM, University of Wollongong, Wollongong, Australia

²Electronic Ceramics Department, Jožef Stefan Institute, Ljubljana, Slovenia

³State Key Lab of New Ceramics and Fine Processing, School of Materials Science and Engineering, Tsinghua University, Beijing, China

⁴Institute of Materials Science, Technische Universität Darmstadt, Darmstadt, Germany

^{a)}Address all correspondence to this author. e-mail: shujun@uow.edu.au

Received: 11 March 2021; accepted: 18 March 2021; published online: 28 March 2021

The year of 2021 is the 100th anniversary of the first publication of ferroelectric behaviour in Rochelle salt, focussing on its piezoelectric properties. Over the past many decades, people witnessed a great impact of ferroelectricity on our everyday life, where numerous ferroelectric materials have been designed and developed to enable the advancement of diverse applications. Now the driving forces for ferroelectric studies stem from regulations on environment, human health and sustainable society development. This leads to the resurgence of lead-free ferroelectric materials for the expectation of replacing the state-of-the-art lead-based counterparts. The next wave of explorations into ferroelectric materials maybe related to the Internet-of-Things, which requires millions of self-powered sensors and memories. This will promote research on ferroelectrics for sensing, energy harvesting and storage, communication and non-volatile memories, from centimetre scale to micro and nanoscale. This review gives a brief discussion from the materials viewpoint, on the challenges and current status of lead-free ferroelectrics based on prospective applications.

Introduction

Ferroelectric materials have diverse functionalities that enable numerous applications, ranging from piezoelectric sensing and dielectric energy storage to electrocaloric solid-state cooling, which have attracted extensive research and development interests. As an important member of the ferroelectric family, perovskite ferroelectric materials play a key role in various kinds of modern electronic devices, such as sensors, transducers and piezoelectric actuators, while relaxor ferroelectrics and antiferroelectrics have great significance for high-power and/or pulse power dielectric energy storage. Critical to environmental concerns and human health, high-performance lead-free ferroelectric materials have given rise to extensive materials research in past decades. In addition to lead-free perovskites, bismuth layer structured ferroelectrics possess good electromechanical properties and high resistivity even at temperatures above 500 °C, making them candidates for high-temperature piezoelectric sensing applications. Meanwhile, the recently discovered

ferroelectricity in fluorite-structured oxides opens a new realm of nanoscale lead-free ferroelectrics for memory application.

Lead-free materials for electromechanical applications

The Pb(Zr,Ti)O₃ (PZT) solid solution and useful outline of its phase diagram were reported in the early 1950s. The milestone studies established the PZT system as well suited for transducer applications with nearly temperature-independent morphotropic phase boundary (MPB). Of vital importance was the exceptional combination of high piezoelectric and electromechanical properties near the MPB compositions [1–3]. The leading position of PZT compositions is due to the strong piezoelectric effect and relatively high Curie temperature. PZTs also allow a wide variation in chemical modification to obtain a broad range of operating parameters without serious reduction of the piezoelectric effect. The chemical dopants include isovalent substitutes of the lead cation by alkaline-earth elements, and

acceptor or donor dopants on the A or B sites, respectively [1–3]. The effects of acceptor or donor doping are attributed to the type of lattice vacancies created to compensate for charge imbalance. That is, oxygen vacancies induced by acceptor dopants inhibit domain wall motion, while lead vacancies induced by donor dopants make domain wall motion easier, leading to “hard” and “soft” characteristics, respectively. A series of formulation-labelled PZTs, have been established to emphasize various properties [4]. In the past, innovations in actuators and ultrasonic transducers have been the main driving forces for new developments in ferroelectric materials. However, the European Union legislation on the Restriction of Hazardous Substances (RoHS) provided a strong driving force to develop the science and technology of lead-free ferroelectric materials [5–16].

KNN-based lead-free piezoceramics with high piezoelectricity

(K,Na)NbO₃-based ((KNN) ceramics are considered to be one of the most promising lead-free ferroelectrics and with the potential to replace PZT [17–21]. It was first reported in the 1950s as a solid solution of KN and NN with an MPB separating two orthorhombic phases or two monoclinic phases. However, applications were limited for KNN ceramics with piezoelectric coefficients of ~100pC/N near the 50/50 MPB composition [9–16]. The resurgence of the research on KNN was accelerated by Saito et al.’s report on textured KNN ceramics with piezoelectric coefficients on the order of 400pC/N [22]. In recent years, the KNN-based system has been extensively studied with gradually increasing piezoelectric properties. Generally, the enhanced piezoelectric activity in KNN ceramics has been attributed to shifting the polymorphic phase transition (PPT) to room temperature, by doping with Li⁺, Sb⁵⁺, and Ta⁵⁺, or the combination of multielements [17–21]. Recent efforts have focussed on the construction of a polymorphic phase boundary, now referred to as the new phase boundary (NPB), which was constructed

by simultaneously shifting both rhombohedral-orthorhombic and orthorhombic-tetragonal phase transition temperatures to, or near, room temperature by adding appropriate dopants, thus achieving much-improved piezoelectricity in multielement-doped KNNs [23–27]. The evolution of the piezoelectric coefficient is plotted as a function of time in Fig. 1a. After 2013, there was a series of breakthroughs resulting in increased d_{33} by constructing the NPB and optimizing the composition design as reported by Wu et al. and others, with d_{33} values above 600pC/N, KNN ceramics are now comparable to “soft” PZTs [27]. More recently, it was proposed that the average macroscopic tetragonal phase together with a large amount of local structure heterogeneities with low angle polar vector (the angle between the local polar vector and average spontaneous polarization direction is < 20°) contributed to the enhanced piezoelectricity and good thermal stability in multielement-doped KNN-based systems, as shown in Fig. 2. Phase field modelling confirmed that the local structure with low angle polar vector can easily rotate under applied electric field because of the competition between the Landau energy barrier and interfacial energies [28].

Single-crystal growth has been explored as a means to improve the piezoelectric properties of lead-free materials, because, as shown for lead-based ferroelectrics, single crystals generally possess much higher dielectric and piezoelectric properties than their polycrystalline counterparts [29]. For example, the piezoelectric coefficients of Pb(Mg_{1/3}Nb_{2/3})O₃-PbTiO₃ (PMN-PT) ceramics are ~500–800 pC/N but d_{33} are > 1500 pC/N in single-crystal form and the electromechanical coupling factors are > 0.9 versus ~0.78–0.8 of polycrystalline ceramics. Besides the excellent piezoelectric properties, ferroelectric single crystals show strong anisotropic behaviour, depending on the engineered domain configurations, due to the variation of symmetries and poling directions. The strong anisotropic behaviour and simplified microstructure in single crystals (i.e. no grain boundaries) benefit the properties and make it possible

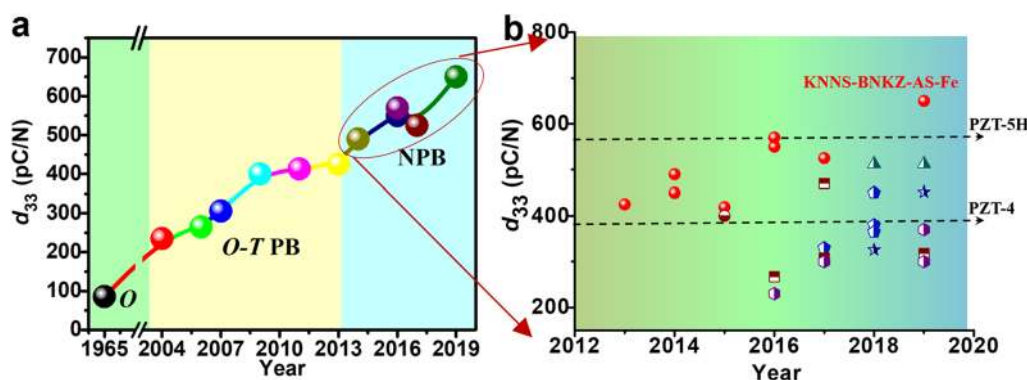


Figure 1: Evolution of piezoelectric coefficients in KNN-based ceramics as a function of year, with focus on the recently developed new phase boundary systems. (the data were adapted from Ref [27]. Copyright 2020 Royal Society of Chemistry).

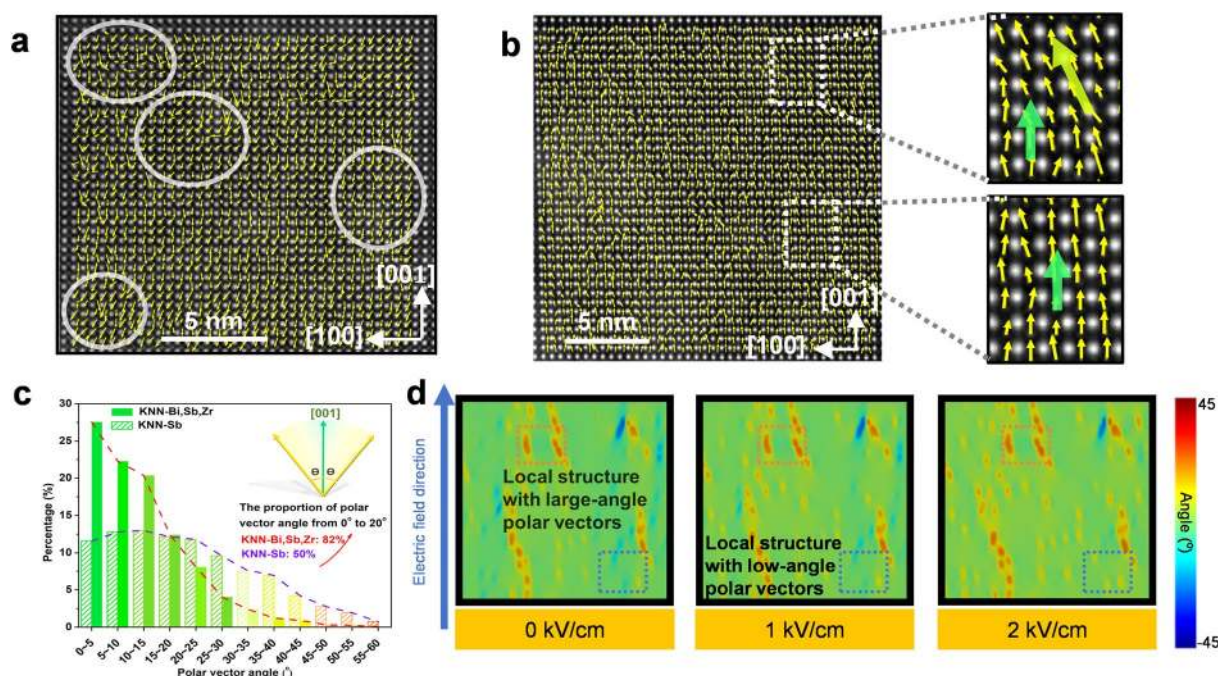


Figure 2: Comparison of the polar vectors in doped KNN ceramics, polar vector map for (a) single element-doped KNN, polar vector along [001] direction is of the spontaneous polarization of tetragonal phase while the polar vector along the diagonal direction is the orthorhombic phase; (b) polar vector map for multielement-doped KNN; (c) the statistical percentage of polar vectors as a function of the polar vector angle (the angle of deviation of the polar vector off the [001] direction); (d) phase field modelling of the microstructure evolution as a function of applied field along [001] direction for average tetragonal phase with local structure heterogeneities. (the data were adapted from Ref. [28]).

to improve the device performance greatly from the application viewpoint.

Relaxor-ferroelectric single crystals exhibit unrivalled, ultrahigh strain and piezoelectric coefficients. The production costs and growth difficulties of these materials are outweighed by the significant advantages in their properties for high-end applications. On the other hand, polycrystalline materials are disadvantaged by the presence of grain boundaries as each randomly oriented grain is typically constrained by its neighbour during domain switching, creating a depolarising field [29]. KNN single crystals have been produced using the Bridgman, high-temperature flux and top seeded solution growth techniques, but with limited success in achieving centimetre size high-quality crystals [29–32]. An alternative approach to develop single crystals is the solid-to-solid transformation of a polycrystalline ceramic to a crystal, i.e. solid-state crystal growth (SSCG). KNN-based single crystals have been grown using a KTaO_3 seed crystal, or by seed-free method (SFSSCG), where the SFSSCG crystals with centimetre size were achieved, but they had high dielectric loss and inferior compositional uniformity [33–38]. The addition of CuO is beneficial for SFSSCG growth of KNN-based crystals because it decreases the width of ferroelectric domains of the crystals. In particular, CuO doping significantly reduces the dielectric loss of the crystals, where the leakage behaviour of the crystals indicates

that the main electrical conduction mechanism is the space-charge-limited-current (SCLC) [39].

The SSCG method reduces the costs associated with single-crystal fabrication compared to solution growth processes and avoids compositional gradients in the grown crystal but the issue of small seed crystals and porosity in the achieved crystals limit potential use of this approach for large-scale single-crystal fabrication and application. Textured lead-based ceramics and lead-free ceramics have better piezoelectric properties than their randomly oriented ceramic counterparts and are comparable, in some cases, to single crystals [40, 41]. High-quality textured ceramics with grains aligned in a crystallographic direction can be produced via the templated grain growth (TGG) [40, 41] or reactive templated grain growth (RTGG) [42]. The textured ceramics have a single-crystal-like nature with respect to the orientation of the crystal axis, hence an enhancement of piezoelectric response has been reported [43–46]. Using these methods, fabrication is relatively easier than single-crystal growth. Textured ceramics have the same ∞m symmetry as that of random ceramics after polarization due to grain orientation in the textured ceramics, generally along the crystallographic [001] direction like that of the template seed. That is, each grain is along [001] direction and poled along [001], and, thus the overall piezoelectric properties are not statistically averaged by the randomly oriented grains as observed in random ceramics.

However, analogous to ceramics with random grain orientation, the existence of grain boundaries generates a depolarization electric field and impedes the domain movement around the boundaries. Hence, the piezoelectric properties are slightly lower than that of single-crystal counterparts [43–47]. KNN-based textured ceramics have been reported by using NaNbO_3 as template seed, yielding a high piezoelectric charge coefficient of 416 pC/N in $(\text{K,Na,Li})(\text{Nb,Ta,Sb})\text{O}_3$ textured ceramics [22], increasing to 700 pC/N by tuning composition in $(\text{K,Na})(\text{Nb,Sb})\text{O}_3\text{-CaZrO}_3\text{-(Bi,K)HfO}_3$, where the piezoelectric strain coefficient is on the order of 980 pm/V [47]. These improvements are due to the contribution from intrinsic piezoelectric anisotropy and large lattice distortion, together with the existence of intermediate monoclinic phase and nanodomain structure [47].

NBT-based lead-free piezoceramics with high mechanical quality factor

High-power piezoelectric materials have been used for a wide range of applications, such as ultrasonic motors and transducers. The figure of merit of piezoelectrics for high-power applications is the product of electromechanical coupling squared and mechanical quality factor ($k^2 Q_m$), which are proportional to the vibration velocity, whereas the mechanical loss is closely related to the heat generation under high vibration. Analogous to PZTs, the compositions of lead-free ferroelectrics have also been tuned to achieve “hard” or “soft” characteristics. While the development of “soft” lead-free piezoelectric ceramics has been of high maturity, the understanding of “hard” lead-free piezoelectric ceramics is still far from satisfactory, leading to a limited chance for high-power applications [48]. An introduction of loss mechanisms and the hardening effect in piezoelectric ceramics, including three different models mainly developed based on the PZT system were reported, as shown in Fig. 3a, including the bulk (or volume) effect, the domain wall effect, and the surface (or grain boundary) effect. The studies on the

hardening behaviour of BaTiO_3 - (BT-) based, $(\text{Na}_{0.5}\text{Bi}_{0.5})\text{TiO}_3$ - (NBT-) based, and KNN-based lead-free piezoelectric ceramics are summarized with emphasis on the approaches to enhance mechanical quality factor [48]. Acceptor modified ferroelectric ceramics featured typical “hardening” characteristics, exhibiting an internal bias field on the order of 0.1–8 kV/cm, as shown in Fig. 3b, this internal bias is due to the domain wall motion being clamped by defect dipoles which is induced by acceptor dopant and oxygen vacancies. Note that mechanical Q_m increases with increasing internal bias field, as depicted in Fig. 3c, demonstrating that the internal bias plays a key role in the high Q_m values. The acceptor-doped NBT-based ceramics show high mechanical Q_m of > 800, comparable to most of the “hard” PZT ceramics [49–51]. Of particular significance is that the “hard” NBT-based lead-free ferroelectrics exhibited minimal variation of the high Q_m under high level vibration velocity, remaining the same at 0.25 m/s, showing great advantage over “hard” PZT ceramics such as PZT4 and PZT8, the Q_m of which was drastically decreased under the same condition. This is because of the high coercive field of NBT-based ceramics (~ 35 kV/cm) is much larger than that of PZTs [52]. The high coercive field is believed to be associated with the distorted oxygen octahedra induced by the A site bismuth cation. Note that a recent concept on hardening of ferroelectrics uses second-phase hardening was proposed, in accordance to second-phase hardening in metals [53].

Lead-free ferroelectrics with broad temperature usage range

The applications of lead-free ferroelectric materials have been limited by temperature usage range. NBT-based lead-free ferroelectrics have higher relaxor to ferroelectric transition temperature than the Curie temperature of BT of $\sim 120^\circ\text{C}$, but their low depolarization temperature $T_d \sim 80\text{--}120^\circ\text{C}$ greatly restricts their application [9–16]. There has been extensive effort to enhance the temperature usage range and improve the thermal stability of

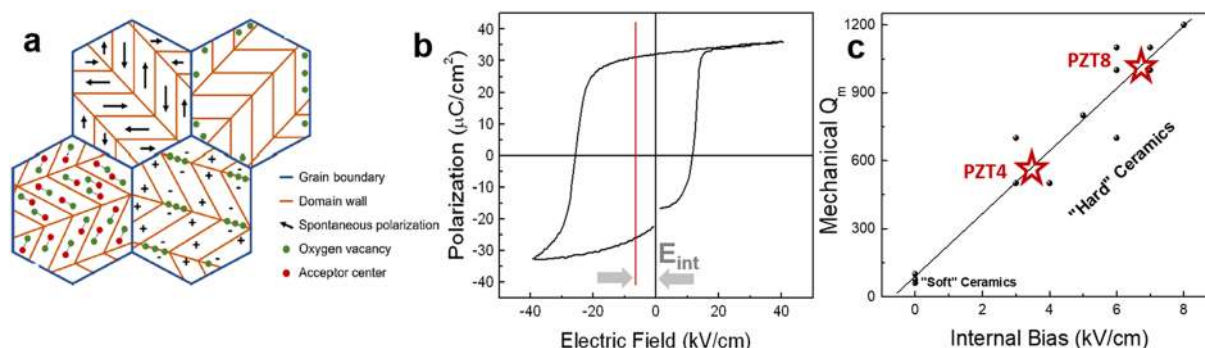


Figure 3: (a) Illustration of three distinctive models of the hardening effect in ferroelectrics (after Ref. [47]); (b) Polarization hysteresis loop exhibiting a strong internal bias field; (c) The relationship between internal bias and mechanical Q_m .

the piezoelectric properties [49, 54–58]. The quenching method has been actively studied in ferroelectric materials to tailor their phase transition behaviour [55–58]. Quenched CuO-doped NBT has a T_d of 143 °C versus 78 °C without quenching and there was no significant deterioration of piezoelectric activity [55–58]. This was also reported in rare-earth Ho-doped NBT–6BT lead-free ceramics, where relatively high piezoelectric performance, as well as an increase of depolarization temperature (T_d), can be realized by thermal quenching. These improvements are attributed to the increased concentration of oxygen vacancies induced by quenching, giving rise to the change of octahedral mode and enhanced lattice distortion, which is beneficial to the temperature stability of piezoelectric properties [59].

In addition to perovskite lead-free ferroelectrics, the bismuth layer (Aurivillius) structure ferroelectrics (BLSF) is another group of ferroelectrics, in which the existence of the $(\text{Bi}_2\text{O}_2)^{2+}$ layers leads to a low dielectric permittivity and high mechanical quality factor perpendicular to the bismuth layers. The high Curie temperature makes BLSFs promising candidates for high-temperature piezoelectric applications. Piezoelectric activity in BLSFs can be further improved by suitable doping, while enhancing the electrical resistivity and achieving a compromise between good polarizability and a high Curie temperature. For example, potassium and cerium co-doped $\text{Bi}_4\text{Ti}_{2.86}\text{W}_{0.14}\text{O}_{12}$ ceramics were reported to possess slightly decreased Curie temperature (T_C) from 632 to 608 °C with increasing dopant level, while both piezoelectricity and resistivity were increased, with maximum d_{33} on the order of 24 pC/N and resistivity of $2.9 \times 10^6 \Omega \text{ cm}$ at 500 °C [60]. On the other hand, the Gd-modified $\text{Ca}_{1-x}\text{Gd}_x\text{Bi}_2\text{Nb}_2\text{O}_9$ BLSF ceramics exhibited very high Curie temperature T_C of 947 °C, with reasonable large piezoelectric d_{33} of 13 pC/N. Of particular significance is that the resistivity was found to be on the order of $2.45 \times 10^7 \Omega \text{ cm}$ at 500 °C, two orders of magnitude higher than that of unmodified ceramics, making the doped $\text{Ca}_{1-x}\text{Gd}_x\text{Bi}_2\text{Nb}_2\text{O}_9$ ceramic great potential for high-temperature piezoelectric sensing applications [61].

Lead-free materials for energy storage applications

Dielectric capacitors have been widely used in numerous fields, such as electronic circuits with various functions (filtering, coupling, decoupling, etc.), microwave communications, hybrid electrical vehicles, distributed power systems, renewable energy storage, and high-power applications [62–66]. For energy storage applications, high energy density, high power density and high energy efficiency are required, so the figure of merit for dielectric materials includes dielectric constant, dielectric breakdown strength and dielectric loss. Linear dielectrics usually possess low permittivity, low dielectric loss and high dielectric

breakdown strength E_b , while the permittivity of non-linear dielectrics varies as a function of electric field. The most promising materials for dielectric energy storage applications are linear dielectric, relaxor ferroelectrics and antiferroelectrics [62–65].

Lead-free relaxor-ferroelectric ceramics

Lead-free-based relaxor ferroelectrics possess the merit of low remanent polarization, high maximum polarization, high breakdown strength and good thermal stability. There have been numerous publications of the dielectric energy storage materials based on relaxor ferroelectrics including SrTiO_3 (ST)-, BT-, NaNbO_3 (NN)-, NBT-based ceramics [67–71]. The bismuth end member has been actively used to form relaxor-ferroelectric solid solutions with ST or BT end member. For example, the addition of $\text{Bi}(\text{Mg}_{0.5}\text{Hf}_{0.5})\text{O}_3$ (BMH) in ST induces relaxor features in the ST-BMH solid solution. A diffuse phase transition was observed in samples with BMH content above 10%, showing typical relaxor characteristic, where 0.8ST–0.2BMH composition exhibits stable dielectric permittivity with variation below 15% over temperature range of –100 to 185 °C, superior to that of undoped ST. A large energy density of 4.1 J/cm³ with high energy efficiency of 92% is obtained at an electric field of 470 kV/cm. Of particular significance is that the energy efficiency remains above 91% at 180 °C [72]. NN-based dielectrics have received much attention for energy storage applications due to their low-cost, lightweight, and nontoxic nature. The hysteresis was successfully reduced by introducing Bi^{3+} and Ti^{4+} into A-site and B-site of NN ceramics, respectively. MnO_2 addition was used to increase the ceramic density and to enhance the cycling reliability. As a result, a high recoverable energy density of 4.3 J/cm³ and a high energy efficiency of 90% were simultaneously achieved in the ceramic capacitor at an applied electric field of 360 kV/cm. Of particular importance is that the ceramic capacitor exhibits stable energy storage properties over a wide temperature range of –70 to 170 °C, with much-improved electric cycling reliability up to 10^5 cycles [73].

Lead-free antiferroelectric ceramics

The merits of antiferroelectrics (AFE) include, but are not limited to, low or zero remanent polarization in AFE phase at low electric field, high spontaneous polarization corresponding to the electric field-induced ferroelectric phase. The two critical electric fields, E_A and E_P , corresponding to the FE-AFE and AFE-FE phase transitions impact the energy efficiency significantly [74–77]. Lead-free antiferroelectric materials have attracted intense research interest with AgNbO_3 (AN) being one of the most attractive candidates. Pure AN ceramics

have an energy storage of $\sim 2 \text{ J/cm}^3$ and a breakdown strength of $< 200 \text{ kV/cm}$. Through proper composition tuning, the breakdown strength can be increased to above 300 kV/cm with the energy density of $4\text{--}5 \text{ J/cm}^3$. The promising dopants in AN-based ceramics include MnO_2 , Ta_2O_5 , Bi_2O_3 , La_2O_3 , or even a small amount of excess Ag_2O [78–85]. Higher energy density can be achieved in AFE with dopant by tailoring the tolerance factor and/or polarizability. However, all the energy efficiencies are quite low at less than 70% due to the hysteresis between AFE-FE and FE-AFE phase transitions. This causes severe issues for practical applications such as thermal breakdown and the volume change during the phase transition can also lead to electromechanical breakdown and result in inferior reliability of cycling [86].

The hysteresis between the phase transitions needs to be decreased to increase the energy efficiency and enhance the cyclic reliability of AFE. Local structure heterogeneity in AFE-based materials smears the AFE-FE phase transitions by forming a solid solution with the relaxor end members

which interrupts the long range AFE ordering. These materials are called relaxor antiferroelectrics, analogous to the relaxor ferroelectrics, as depicted in Fig. 4 [86, 87]. AN- AgTaO_3 (AT) solid solutions with an energy density of 4.2 J/cm^3 but the efficiency was only 69% when the AT content is below 20%, due to the stabilized room temperature AFE M2 phase. With increasing the AT content, the diffused M2-M3 phase transition was shifted to room temperature at 55% AT content. High energy storage density of 6.3 J/cm^3 with high efficiency of 90% was simultaneously achieved at an electric field of 470 kV/cm [88]. Another relaxor AFE NBT- $(\text{Sr}_{0.7}\text{Bi}_{0.2})\text{TiO}_3$ (SBT) solid solution with a high energy density of 9.5 J/cm^3 at 600 kV/cm was achieved in a multilayer ceramic capacitor (MLCC), with dielectric layer thickness of $20 \mu\text{m}$, and the energy efficiency remained above 90% over the entire field range [89]. This can be further increased to 21.5 J/cm^3 with yet high efficiency of 80% in $\langle 111 \rangle$ textured MLCC at 1000 kV/cm , due to the greatly enhanced E_b [90]. Comparisons of the textured and non-textured ceramics are

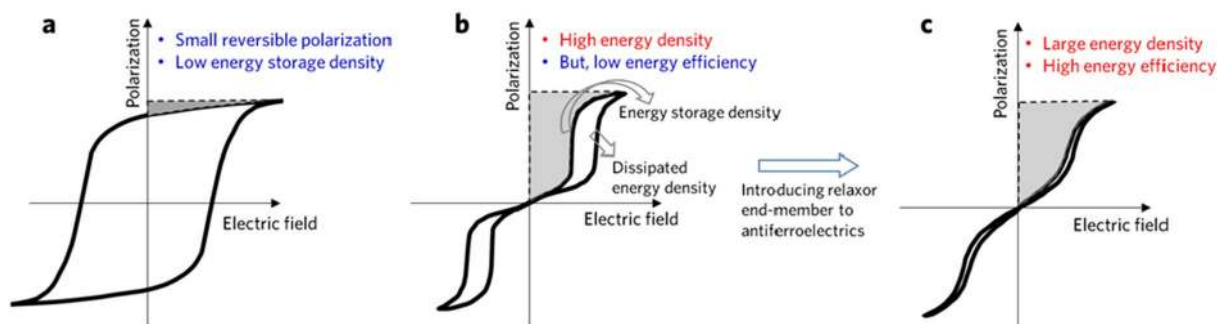


Figure 4: Schematic diagram of energy storage properties for classical ferroelectric, antiferroelectric, and relaxor antiferroelectric materials. (a) The polarization hysteresis loop for a ferroelectric material; (b) polarization hysteresis loop for an antiferroelectric material, where the storage energy density and dissipated energy density are given; (c) Expected polarization hysteresis loop for an antiferroelectric solid solution with a relaxor end member. (adapted from Ref. [86], Copyright 2018 John Wiley and Sons).

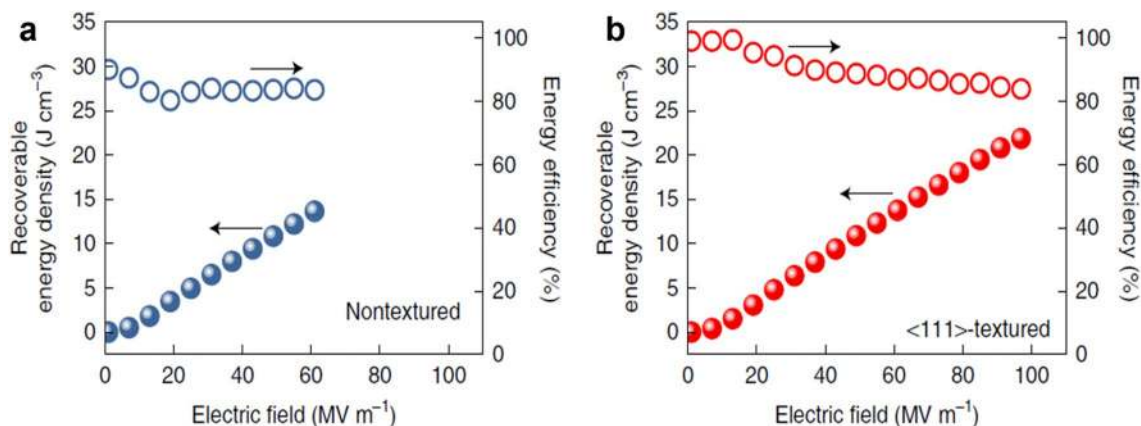


Figure 5: Recoverable energy density and efficiency as a function of the electric field calculated using the P - E loops for the non-textured and the $\langle 111 \rangle$ -textured NBT-SBT multilayer ceramics. (adapted from Ref. [90] Copyright 2020 Springer Nature).

featured in Fig. 5. The $\langle 111 \rangle$ textured ceramics possess low electrostrictive strain because the electrostrictive coefficient along $\langle 111 \rangle$ direction is the lowest in the perovskite structure [91], thus greatly decreasing the electromechanical breakdown probability.

Lead-free materials for other applications

In addition to the extensively studied electromechanical and dielectric energy storage applications, the electrocaloric effect of lead-free ferroelectrics has been revisited [92–97]. The electrocaloric effect, which is the converse to the pyroelectric effect, was discovered in 1930. Being the electrical analogue of the magnetocaloric effect, it is defined as the isothermal entropy or adiabatic temperature change of a dielectric material when an electric field is applied or removed. This has been actively studied in recent years due to its potential solid-state cooling applications, such as efficient refrigeration, air conditioning, and heat pumping. For refrigeration devices, a large temperature change (ΔT) and good temperature stability are required, which are highly related to the phase structure and the applied electric field, the giant electrocaloric effect ($\Delta T_{\text{max}} = 12 \text{ K}$) was reported in PZT thin films. Lead-free ferroelectric electrocaloric ceramics are promising candidates for environment-friendly cooling devices. A diffuse ferroelectric–paraelectric phase transition is formed in KNN by appropriate composition engineering and results in both a large ΔT of 1.24 K at electric field of 65 kV/cm and a high $\Delta T/\Delta E$ of 0.19 K mm/kV, over a broad temperature span exceeding 55 °C. This work not only opens a new strategy for obtaining high-performance lead-free ferroelectrics for solid-state cooling applications, but also extends the application area of the KNN-based lead-free ferroelectrics [98].

The unexpected ferroelectricity reported in doped HfO_2 one decade ago, due to the formation of a noncentrosymmetric orthorhombic phase, has revived the research on complementary metal–oxide–semiconductor (CMOS) compatible ferroelectrics in emerging ferroelectric memory applications [99–102]. The doped/alloyed HfO_2 and ZrO_2 thin films revolutionized not only the field of ferroelectric physics but also various ranges of device applications. Especially when the two oxides are combined in a 1:1 ratio, the ferroelectric polarization of the material became the most distinctive. Many researchers have investigated various process conditions such as controlling $\text{Hf}_{0.5}\text{Zr}_{0.5}\text{O}_2$ (HZO) film thickness and modifying different metal electrodes. By understanding the polarization–electric field (P–E), current–electric field (I–E), and electrical breakdown characteristics of the different samples, it was found that Ar plasma treatment can control the degree of ferroelectric and antiferroelectric phases of HZO films. This sheds light on the engineering of the recently discovered ferroelectric HZO material which has drawn immense attention from material/device engineers [103].

Perspective on lead-free ferroelectric materials

Legislation, including the Waste from Electrical and Electronic Equipment, Restriction of Hazardous Substances and End-of-life Vehicles, has provided a strong driving force for the research of lead-free ferroelectrics over the last two decades. The existing challenges of lead-free, as compared to lead-based ferroelectrics, have brought more attention to the material development, especially considering the very unique properties required for the very diverse applications.

For acoustic transducer applications, the high piezoelectric/electromechanical properties related to the efficiency and bandwidth of the transducer are required, while for high-power transducer applications, in addition to electromechanical properties, the high mechanical Q_m and low loss are required to achieve high power output and low power dissipation. Taking advantage of the strong anisotropy and inherently associated high electromechanical coupling of single crystals, more research has focussed on single-crystal growth and textured ceramics in the KNN-based lead-free system. NBT-based lead-free piezoceramics are promising for high-power applications because of their high coercive field which guarantees high drive field stability, where the mechanical Q_m remains at high values under hard drive condition. On the other hand, for dielectric energy storage capacitor application, medium dielectric permittivity and high breakdown strength are important factors impacting energy density, while leakage current, dielectric loss and phase transition hysteresis are closely associated with the energy efficiency and reliability of the capacitors. The general operating temperature range of most electronic devices is between -50 to $150 \text{ }^\circ\text{C}$, which requires high thermal stability of the properties and demands that the phase transition temperature, or depolarization temperature, are outside of the usage temperature range. Thermal quenching is an effective way to impact the phase transition behaviour thus expanding the temperature usage range, while forming solid solutions and utilizing composites have also been actively studied. For energy storage application, introducing the relaxor component or local structure heterogeneity has been studied, which is found to smear the phase transition or broaden the temperature usage range with high stability and reliability. In addition, for high-temperature sensing applications up to $1000 \text{ }^\circ\text{C}$, the electrical resistivity at elevated temperature is the most important consideration.

Last but not the least, multilayer lead-free ferroelectrics form an extremely important direction for real applications, which is expected to greatly enhance properties. This includes the multilayer actuators to achieve large displacement at low driving electric field [104–106], while the multilayer capacitors are important for both energy storage and electrocaloric applications [107, 108]. Given that the dielectric breakdown

strength scales inversely with dielectric layer thickness, the multilayer capacitor can withstand ultrahigh electric fields, thus high energy storage density or large electrocaloric entropy change. Due to the fact that both multilayer actuators and multilayer capacitors are co-fired with electrodes, it is interesting to study the co-sintering behaviour of lead-free ferroelectrics. For example, low-temperature firing of KNN multilayers with base metal electrode (such as Cu or Ni) in reducing atmosphere has been actively pursued in both academia and industry, revealing promising results [105, 106]. Hence, this provides a good paradigm for transferring material research to real usage of lead-free ferroelectrics.

Acknowledgments

Shujun Zhang acknowledges the support of ARC (FT140100698). Jing-Feng Li thanks the Tsinghua University Spring Breeze Fund (Grant No. 2020Z99CFZ026) and Tsinghua-Foshan Innovation Special Fund (TFISF) (Grant No. 2020THFS0113). Barbara Malič thanks the Slovenian Research Agency (P2-0105, J2-2497). Jürgen Rödel thanks the Funding by the state of Hesse through the LOEWE project “FLAME”. The authors thank Gary Messing for his suggestions in this paper.

Data availability

Data can be provided upon requesting of the authors.

Declarations

Conflict of interest On behalf of all authors, the corresponding author states that there is no conflict of interest.

References

1. E. Sawaguchi, Ferroelectricity versus antiferroelectricity in the solid solutions of PZ and PT. *J. Phys. Soc. Jpn.* **8**, 615 (1953)
2. G. Shirane, K. Suzuki, Crystal structure of $\text{Pb}(\text{Zr}, \text{Ti})\text{O}_3$. *J. Phys. Soc. Jpn.* **7**, 5 (1952)
3. B. Jaffe, R. Roth, S. Marzullo, Piezoelectric properties of lead zirconate-lead titanate solid-solution ceramics. *J. Appl. Phys.* **25**, 809 (1954)
4. S. Trolrier-McKinstry, S. Zhang, A.J. Bell, X. Tan, High performance piezoelectric crystals, ceramics and films. *Ann. Rev. Mater. Res.* **48**, 191 (2018)
5. A.J. Bell, O. Deubzer, Lead-free piezoelectrics- The environmental and regulatory issues. *MRS Bull.* **43**, 581 (2018)
6. J.F. Li, *Lead-Free Piezoelectric Materials* (Wiley, Weinheim, Germany, 2021)
7. S. Priya, S. Nahm, *Advances Lead-Free Piezoelectrics* (Springer Science, New York, 2012)
8. J.G. Wu, *Advances in lead-free piezoelectric materials* (Springer Nature, Singapore, 2018)
9. J. Rodel, W. Jo, K.T.P. Seifert et al., Perspective on the development of lead-free piezoceramics. *J. Am. Ceram. Soc.* **92**, 1153 (2009)
10. T.R. Shrout, S. Zhang, Lead-free piezoelectric ceramics: alternatives for PZT? *J. Electroceram.* **19**, 111 (2007)
11. J. Rodel, K.G. Webber, R. Dittmer et al., Transferring lead-free piezoelectric ceramics into application. *J. Europ. Ceram. Soc.* **35**, 1659 (2015)
12. W. Jo, R. Dittmer, M. Acosta et al., Giant electric field induced strains in lead-free ceramics for actuator applications- status and perspective. *J. Electroceram.* **29**, 71 (2012)
13. J. Koruza, A.J. Bell, T. Fromling et al., Requirements for the transfer of lead-free piezoceramics into application. *J. Materiomics* **4**, 13 (2018)
14. M.D. Maeder, D. Damjanovic, N. Setter, Lead free piezoelectric materials. *J. Electroceram.* **13**, 385 (2004)
15. J. Rodel, J.F. Li, Lead-free piezoceramics: status and perspectives. *MRS Bull.* **43**, 576 (2018)
16. C.H. Hong, H.P. Kim, B.Y. Choi et al., Lead-free piezoceramics-where to move on? *J. Materiomics* **2**, 1 (2016)
17. J.F. Li, K. Wang, F.Y. Zhu et al., KNN-based lead-free piezoceramics: fundamental aspects, processing technologies and remaining challenges. *J. Am. Ceram. Soc.* **96**, 3677 (2013)
18. J. Wu, D. Xiao and J. Zhu. Potassium sodium niobate lead-free piezoelectric materials: past, present and future of phase boundaries. 115, 2559 (2015).
19. K. Xu, J. Li, X. Lv et al., Superior piezoelectric properties in potassium-sodium niobate lead-free ceramics. *Adv. Mater.* **28**, 8519 (2016)
20. K. Wang, F.Z. Yao, W. Jo et al., Temperature-insensitive KNN based lead-free piezoactuator ceramics. *Adv. Funct. Mater.* **23**, 4079 (2013)
21. B. Malič, J. Koruza, J. Hrescak et al., Sintering of lead-free piezoelectric sodium potassium niobate ceramics. *Materials* **8**, 8117 (2015)
22. Y. Saito, H. Takao, T. Tani et al., Lead-free piezoceramics. *Nature* **432**, 84 (2004)
23. R. Wang, H. Bando, T. Katsumata et al., Tuning the orthorhombic-rhombohedral phase transition temperature in sodium potassium niobate by incorporating barium zirconate. *Phys. Status Solidi: Rapid Res. Lett.* **3**, 142 (2009)
24. R. Wang, H. Bando, M. Kidate et al., Effects of A-site ions on the phase transition temperatures and dielectric properties of NKN-AZrO₃ solid solutions. *Jpn. J. Appl. Phys.* **50**, 09ND10 (2011)
25. R. Zuo, J. Fu, D. Lv, Phase transformation and tunable piezoelectric properties of lead-free (Na, K, Li)(Nb, Sb, Ta)O₃ system. *J. Am. Ceram. Soc.* **92**, 283 (2009)

26. J. Fu, R. Zuo, Structural evidence for the polymorphic phase boundary in NKN based perovskites close to the rhombohedral-tetragonal phase coexistence zone. *Acta Mater.* **195**, 571 (2020)
27. X. Lv, J.G. Zhu, D.Q. Xiao et al., Emerging new phase boundary in potassium sodium niobate based ceramics. *Chem. Soc. Rev.* **49**, 671 (2020)
28. X. Gao, Z. Cheng, Z. Chen et al., The mechanism for the enhanced piezoelectricity in mult-elements doped KNN ceramics. *Nat. Commun.* **12**, 881 (2021)
29. P. Kabakov, C. Dean, V. Kurusingal et al., Solid-state crystal growth of lead-free ferroelectrics. *J. Mater. Chem. C*, **8**, 7606 (2020)
30. C. Hu, X. Meng, M.H. Zhang et al., Ultra-large electric field induced strain in potassium sodium niobate crystals. *Sci. Adv.* **6**, eaay5979 (2020)
31. H. Liu, P. Veber, J. Rodel et al., High performance piezoelectric (K, Na, Li)(Nb, Ta, Sb)O₃ single crystals by oxygen annealing. *Acta Mater.* **148**, 499 (2018)
32. K. Chen, G. Xu, D. Yang, X. Wang, Dielectric and piezoelectric properties of lead-free KNN-LN crystals grown by the Bridgman method. *J. Appl. Phys.* **101**, 044103 (2007)
33. S.Y. Ko, J.H. Park, I.W. Kim et al., Improved solid-state conversion and piezoelectric properties of NBT-BT-KNN single crystals. *J. Europ. Ceram. Soc.* **37**, 407 (2017)
34. J.G. Fisher, A. Bencan, M. Kosec et al., Growth of dense single crystals of potassium sodium niobate by a combination of solid-state crystal growth and hot pressing. *J. Am. Ceram. Soc.* **91**, 1503 (2008)
35. M. Jiang, C.A. Randall, H. Guo et al., Seed-free solid-state growth of large lead-free piezoelectric single crystals: NKN. *J. Am. Ceram. Soc.* **98**, 2988 (2015)
36. C.W. Ahn, H.Y. Lee, G. Han et al., Self-growth of centimetre scale single crystals by normal sintering process in modified potassium sodium niobate ceramics. *Sci. Rep.* **5**, 17656 (2015)
37. C.W. Ahn, A. Rahman, J. Ryu et al., Composition design for growth of single crystal by abnormal grain growth in modified potassium sodium niobate ceramics. *Cryst. Growth Des.* **16**, 6586 (2016)
38. I. Fujii, S. Ueno, S. Wada, Effects of sintering aid and atmosphere powder on the growth of KNN single crystals fabricated by solid-state crystal growth method. *J. Europ. Ceram. Soc.* **40**, 2970 (2020)
39. X. Yao, M. Jiang, S. Han et al., Microstructure and electrical properties of CuO-doped K_{0.5}Na_{0.5}NbO₃-based single crystals with low dielectric loss. *J. Mater. Res.* **20**, 21 (2021). <https://doi.org/10.1557/s43578-020-00015-2>
40. G.L. Messing, S. Trolier-McKinstry, E.M. Sabolsky et al., Templated grain growth of textured piezoelectric ceramics. *Crit. Rev. Solid State Mater. Sci.* **29**, 45 (2004)
41. G.L. Messing, S.F. Poterala, Y.F. Chang et al., Texture-engineered ceramics—property enhancements through crystallographic tailoring. *J. Mater. Res.* **32**, 3219 (2017)
42. T. Tani, T. Kimura, Reactive-templated grain growth processing for lead free piezoelectric ceramics. *Adv. Appl. Ceram.* **105**, 55 (2006)
43. E.M. Sabolsky, A.R. James, S. Kwon et al., Piezoelectric properties of <001> textured PMN-PT ceramics. *Appl. Phys. Lett.* **78**, 2551 (2001)
44. S. Yang, J. Li, Y. Liu et al., Textured ferroelectric ceramics with high electromechanical coupling factors over a broad temperature range. *Nat. Commun.* **12**, 1414 (2021)
45. A.D. Moriana, S. Zhang, Lead-free textured piezoceramics using tape casting: a review. *J. Materiomics*, **4**, 277 (2018)
46. E.M. Sabolsky, S. Trolier-McKinstry, G.L. Messing, Dielectric and piezoelectric properties of <001> fiber-textured 0675PMN-0325PT ceramics. *J. Appl. Phys.* **93**, 4072 (2003)
47. P. Li, J.W. Zhai, B. Shen et al., Ultrahigh piezoelectric properties in textured KNN-based lead-free ceramics. *Adv. Mater.* **30**, 1705171 (2018)
48. T.N. Nguyen, H.C. Thong, Z.X. Zhu et al., Hardening effect in lead-free piezoelectric ceramics. *J. Mater. Res.* (2021). <https://doi.org/10.1557/s43578-020-00016-1>
49. K.V. Lalitha, T. Zhu, M.P. Salazar et al., Influence of Zn-doping on ferroelectric stability and electromechanical hardening in (Na_{1/2}Bi_{1/2})/TiO₃-BaTiO₃. *J. Amer. Ceram. Soc.* **104**, 2021 (2021)
50. Y. Doshida, H. Shimizu, Y. Mizuno, H. Tamura, Investigation of high power properties of (Bi, Na, Ba)TiO₃ and (Sr, Ca)₂NaNb₅O₁₅ piezoelectric ceramics. *Jpn. J. Appl. Phys.* **52**, 0701 (2013)
51. T. Watanabe, Y. Hiruma, H. Nagaata, T. Takenaka, High power characteristics at large amplitude vibration of BNT-based lead-free ferroelectric ceramics. *Ferroelectrics* **385**, 135 (2009)
52. H.J. Lee, S.O. Ural, L. Chen et al., High power characteristics of lead-free piezoelectric ceramics. *J. Am. Ceram. Soc.* **95**, 3383 (2012)
53. K.V. Lalitha, L. Riemer, J. Koruza, J. Rödel, Hardening of electromechanical properties in piezoceramics using a composite approach. *Appl. Phys. Lett.* **111**, 022905 (2017)
54. L. Riemer, L.K. Venkataraman, X. Jiang et al., Stress-induced phase transition in lead-free relaxor ferroelectric composites. *Acta Mater.* **136**, 271 (2017)
55. H. Muramatsu, H. Nataga, T. Takenaka, Quenching effects for piezoelectric properties on lead-free BNT ceramics. *Jpn. J. Appl. Phys.* **55**, 10TB07 (2016)
56. Q. Li, J. Wei, T. Tu et al., Remarkable piezoelectricity and stable high-temperature dielectric properties of quenched BF-BT ceramics. *J. Am. Ceram. Soc.* **100**, 5573 (2017)

57. J. Chen, J. Cheng, J. Guo et al., Excellent thermal stability and aging behaviors in BF-BT piezoelectric ceramics with rhombohedral phase. *J. Am. Ceram. Soc.* **103**, 374 (2020)
58. S. Harada, Y. Takagi, H. Nagata et al., Quenching effects on electrical properties of Cu-doped $(\text{Bi}_{1/2}\text{Na}_{1/2})\text{TiO}_3$ -based solid solution ceramics. *J. Mater. Res.* (2021). <https://doi.org/10.1557/s43578-020-00048-7>
59. L. Zheng, C. Chen, X. Jiang et al., Effects of defect on thermal stability and photoluminescence in quenched Ho-doped $0.94\text{Na}0.5\text{Bi}0.5\text{TiO}_3\text{--}0.06\text{BaTiO}_3$ lead-free ceramics. *J. Mater. Res.* (2021). <https://doi.org/10.1557/s43578-020-00076-3>
60. Z. Shen, Z. Zhang, C. Qin et al., Effect of $(\text{K}_{0.5}\text{Ce}_{0.5})$ complex on the electrical properties of lead-free $\text{Bi}_4\text{Ti}_{2.86}\text{W}_{0.14}\text{O}_{12}$ high-temperature piezoelectric ceramics. *J. Mater. Res.* (2021). <https://doi.org/10.1557/s43578-020-00078-1>
61. J.N. Chen, C. Kang, R.M. Hou et al., Dielectric, ferroelectric, and piezoelectric properties of Gd-modified $\text{CaBi}_2\text{Nb}_2\text{O}_9$ high Curie temperature ceramics. *J. Mater. Res.* (2021). <https://doi.org/10.1557/s43578-020-00023-2>
62. L. Yang, X. Kong, F. Li et al., Perovskite lead-free dielectrics for energy storage applications. *Prog. Mater. Sci.* **102**, 72 (2019)
63. Z. Yao, Z. Song, H. Hao et al., Homogeneous/inhomogeneous structured dielectric and their energy storage performances. *Adv. Mater.* **29**, 1601727 (2017)
64. G. Wang, J. Li, X. Zhang et al., Ultrahigh energy storage density lead-free multilayers by controlled electrical homogeneity. *Energy Environ. Sci.* **12**, 582 (2019)
65. H. Zhang, T. Wei, Q. Zhang et al., A review on the development of lead-free ferroelectric energy-storage ceramics and multilayer capacitors. *J. Mater. Chem. C* **8**, 16648 (2020)
66. S.I. Shkuratov, J. Baird, V.G. Antipov, S. Zhang, J.B. Chase, Multilayer PZT 95/5 Antiferroelectric Film Energy Storage Devices with Giant Power Density. *Adv. Mater.* **31**, 1904819 (2019)
67. H. Ogihara, C. Randall, S. Trolier-McKinstry, High-energy density capacitors utilizing $\text{BaTiO}_3\text{--BiScO}_3$ ceramics. *J. Am. Ceram. Soc.* **92**, 1719 (2009)
68. L. Yang, X. Kong, Z. Cheng et al., Enhanced energy storage performance of sodium niobate-based relaxor dielectrics by a ramp-to-spike sintering profile. *ACS Appl. Mater. Interfaces* **12**, 32834 (2020)
69. Z. Yang, H. Du, S. Qu et al., Significantly enhanced recoverable energy storage density in potassium-sodium niobate-based lead free ceramics. *J. Mater. Chem. A* **4**, 13778 (2016)
70. X. Jiang, H. Hao, S. Zhang et al., Enhanced energy storage and fast discharge properties of BT based ceramics modified by BMZ. *J. Europ. Ceram. Soc.* **39**, 1103 (2019)
71. Z. Shen, X. Wang, B. Luo et al., $\text{BaTiO}_3\text{--BiYbO}_3$ perovskite materials for energy storage applications. *J. Mater. Chem. A* **3**, 18146 (2015)
72. X. Kong, L. Yang, Z. Cheng et al., $\text{Bi}(\text{Mg}_{0.5}\text{Hf}_{0.5})\text{O}_3$ -modified SrTiO_3 lead-free ceramics for high-temperature energy storage capacitors. *J. Mater. Res.* **20**, 21 (2021). <https://doi.org/10.1557/s43578-020-00007-2>
73. L. Yang, X. Kong, Z. Cheng et al., Enhanced energy density and electric cycling reliability via MnO_2 modification in sodium niobate-based relaxor dielectric capacitors. *J. Mater. Res.* (2021). <https://doi.org/10.1557/s43578-020-00085-2>
74. X. Tan, C. Ma, J. Frederick et al., The antiferroelectric ferroelectric phase transition in lead-containing and lead-free perovskite ceramics. *J. Am. Ceram. Soc.* **94**, 283 (2011)
75. X.H. Hao, J.W. Zhai, L.B. Kong, Z. Xu, A comprehensive review on the progress of lead zirconate based antiferroelectric materials. *Prog. Mater. Sci.* **63**, 1 (2014)
76. J. Gao, Q. Li, S. Zhang, J.F. Li, Lead-free antiferroelectric AgNbO_3 : phase transitions and structure engineering for dielectric energy storage applications. *J. Appl. Phys.* **128**, 070903 (2020)
77. D. Yang, J. Gao, L. Shu et al., Lead-free antiferroelectric niobates AgNbO_3 and NaNbO_3 for energy storage applications. *J. Mater. Chem. A* **8**, 23724 (2020)
78. L. Zhao, Q. Liu, S. Zhang, J. Li, Lead-free AN antiferroelectric ceramics with an enhanced energy storage performance using MnO_2 modification. *J. Mater. Chem. C* **4**, 8380 (2016)
79. L. Zhao, J. Gao, Q. Liu et al., Silver niobate lead-free antiferroelectric ceramics: enhancing energy storage density by B-site doping. *ACS Appl. Mater. Interfaces* **10**, 819 (2018)
80. Y. Tian, L. Jin, H. Zhang et al., High energy density in silver niobate ceramics. *J. Mater. Chem. A* **4**, 17279 (2016)
81. Y. Tian, L. Jin, H. Zhang et al., Phase transitions in bismuth modified silver niobate ceramics for high power energy storage. *J. Mater. Chem. A* **5**, 17525 (2017)
82. J. Gao, L. Zhao, K. Lee et al., Enhanced antiferroelectric phase stability in La-doped AN: perspectives from the microstructure to energy storage property. *J. Mater. Chem. A* **7**, 2225 (2019)
83. N. Luo, K. Han, F. Zhuo et al., Aliovalent A-site engineered AN lead-free antiferroelectric ceramics toward superior energy storage density. *J. Mater. Chem. A* **7**, 14118 (2019)
84. L. Zhao, Q. Liu, J. Gao et al., Lead-free antiferroelectric silver niobate tantalate with high energy storage performance. *Adv. Mater.* **29**, 1701824 (2017)
85. N. Luo, X. Tang, K. Han et al., Silver stoichiometry engineering: an alternative way to improve energy storage density of AgNbO_3 -based antiferroelectric ceramics. *J. Mater. Res.* (2021). <https://doi.org/10.1557/s43578-020-00018-z>
86. F. Li, S. Zhang, D. Damjanovic et al., Local structural heterogeneity and electromechanical responses of ferroelectrics: learning from relaxor ferroelectrics. *Adv. Funct. Mater.* **28**, 1801504 (2018)
87. H. Qi, R. Zuo, A. Xie et al., Ultrahigh energy storage density in NN-based lead-free relaxor antiferroelectric ceramics with nanoscale domains. *Adv. Funct. Mater.* **19**, 1903877 (2019)

88. N. Luo, K. Han, M. Cabral et al., Constructing phase boundary in AgNbO₃ antiferroelectrics: pathway simultaneously achieving high energy density and efficiency. *Nat. Commun.* **11**, 4824 (2020)
89. J. Li, F. Li, Z. Xu et al., Multilayer lead-free ceramic capacitors with ultrahigh energy density and efficiency. *Adv. Mater.* **30**, 1802155 (2018)
90. J. Li, Z. Shen, X. Chen et al., Grain-orientation-engineered multilayer ceramic capacitors for energy storage applications. *Nature Mater.* **19**, 999 (2020)
91. F. Li, L. Jin, X. Xu et al., Electrostrictive effect in ferroelectrics: an alternative approach to improve piezoelectricity. *Appl. Phys. Rev.* **1**, 011103 (2014)
92. A.S. Mischenko, Q.M. Zhang, J.F. Scott et al., Giant electrocaloric effect in thin-film PbZr_{0.95}Ti_{0.05}O₃. *Science* **311**, 1270 (2006)
93. S. Lu, Q.M. Zhang, Electrocaloric materials for solid-state refrigeration. *Adv. Mater.* **21**, 1983 (2009)
94. B. Rozic, M. Kosec, H. Ursic et al., Influence of the critical point on the electrocaloric response of relaxor ferroelectrics. *J. Appl. Phys.* **110**, 064118 (2011)
95. U. Plaznik, M. Vrabelj, Z. Kutnjak et al., Electrocaloric cooling: The importance of electric-energy recovery and heat regeneration. *EPL* **111**, 57009 (2015)
96. X. Wang, J. Wu, B. Dkhil et al., Enhanced electrocaloric effect near polymorphic phase boundary in lead-free potassium sodium niobate ceramics. *Appl. Phys. Lett.* **110**, 063904 (2017)
97. Z. Luo, D. Zhang, Y. Liu et al., Enhanced electrocaloric effect in lead-free BaTiSnO₃ ceramics near room temperature. *Appl. Phys. Lett.* **105**, 102904 (2014)
98. N. Zhang, T. Zheng, C. Zhao et al., Enhanced electrocaloric effect in compositional driven potassium sodium niobate-based relaxor ferroelectrics. *J. Mater. Res.* (2021). <https://doi.org/10.1557/s43578-020-00081-6>
99. T.S. Boscke, J. Muller, D. Brauhaus et al., Ferroelectricity in hafnium oxide thin films. *Appl. Phys. Lett.* **99**, 102903 (2011)
100. T.S. Böske, D. Bräuhäus et al., Phase transitions in ferroelectric silicon doped hafnium oxide. *Appl. Phys. Lett.* **99**, 112904 (2011)
101. J.Y. Park, K. Yang, D.H. Lee et al., A perspective on semiconductor devices based on fluorite-structured ferroelectrics from the materials-device integration perspective. *J. Appl. Phys.* **128**, 240904 (2020)
102. E.T. Breyer, H. Mulaosmannovic, T. Mikolajick, S. Slesazeck, Perspective on ferroelectric, hafnium oxide based transistors for digital beyond von-Neumann computer. *Appl. Phys. Lett.* **118**, 050501 (2021)
103. J. Hur, P. Wang, N. Tasneem et al., Exploring argon plasma effect on ferroelectric Hf_{0.5}Zr_{0.5}O₂ thin film atomic layer deposition. *J. Mater. Res.* (2021). <https://doi.org/10.1557/s43578-020-00074-5>
104. C. Randall, A. Kelnberger, G. Yang et al., High strain piezoelectric multilayer actuators - a material science and engineering challenge. *J. Electroceram.* **14**, 177 (2005)
105. L. Gao, H. Guo, S. Zhang, C. Randall, Based metal co-fired multilayer piezoelectrics. *Actuators* **5**, 8 (2016)
106. K. Kobayashi, Y. Doshida, Y. Mizuno, C. Randall, Possibility of cofiring a nickel inner electrode in a NKN-LiF piezoelectric actuator. *Jpn. J. Appl. Phys.* **52**, 09KD07 (2013)
107. G. Wang, Z. Lu, J. Li et al., Lead-free (Ba, Sr)TiO₃ based multilayer ceramic capacitors with high energy density. *J. Europ. Ceram. Soc.* **40**, 1779 (2020)
108. H. Yang, W. Bao, Z. Lu et al., High-energy storage performance in BaTiO₃-based lead-free multilayer ceramic capacitors. *J. Mater. Res.* (2021). <https://doi.org/10.1557/s43578-020-00093-2>